

STONE AGE INSTITUTE PUBLICATION SERIES

Series Editors Kathy Schick and Nicholas Toth

Stone Age Institute
Gosport, Indiana
and
Indiana University,
Bloomington, Indiana

Number 1.

THE OLDOWAN: Case Studies into the Earliest Stone Age
Nicholas Toth and Kathy Schick, editors

Number 2.

BREATHING LIFE INTO FOSSILS:
Taphonomic Studies in Honor of C.K. (Bob) Brain
Travis Rayne Pickering, Kathy Schick, and Nicholas Toth, editors

Number 3.

THE CUTTING EDGE:
New Approaches to the Archaeology of Human Origins
Kathy Schick, and Nicholas Toth, editors

Number 4.

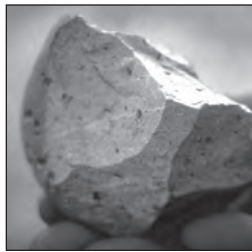
THE HUMAN BRAIN EVOLVING:
Paleoneurological Studies in Honor of Ralph L. Holloway
Douglas Broadfield, Michael Yuan, Kathy Schick and Nicholas Toth, editors

STONE AGE INSTITUTE PUBLICATION SERIES
NUMBER 1

THE OLDOWAN:

Case Studies Into the Earliest Stone Age

Edited by Nicholas Toth and Kathy Schick



Stone Age Institute Press · www.stoneageinstitute.org
1392 W. Dittmore Road · Gosport, IN 47433

COVER PHOTOS

Front, clockwise from upper left:

- 1) *Excavation at Ain Hanech, Algeria (courtesy of Mohamed Sahnouni).*
- 2) *Kanzi, a bonobo ('pygmy chimpanzee') flakes a chopper-core by hard-hammer percussion (courtesy Great Ape Trust).*
- 3) *Experimental Oldowan flaking (Kathy Schick and Nicholas Toth).*
- 4) *Scanning electron micrograph of prehistoric cut-marks from a stone tool on a mammal limb shaft fragment (Kathy Schick and Nicholas Toth).*
- 5) *Kinesiological data from Oldowan flaking (courtesy of Jesus Dapena).*
- 6) *Positron emission tomography of brain activity during Oldowan flaking (courtesy of Dietrich Stout).*
- 7) *Experimental processing of elephant carcass with Oldowan flakes (the animal died of natural causes). (Kathy Schick and Nicholas Toth).*
- 8) *Reconstructed cranium of Australopithecus garhi. (A. garhi, BOU-VP-12/130, Bouri, cranial parts, cranium reconstruction; original housed in National Museum of Ethiopia, Addis Ababa. ©1999 David L. Brill).*
- 9) *A 2.6 million-year-old trachyte bifacial chopper from site EG 10, Gona, Ethiopia (courtesy of Sileshi Semaw).*

Back:

Photographs of the Stone Age Institute. Aerial photograph courtesy of Bill Oliver.

Published by the Stone Age Institute.
ISBN-10: 0-9792-2760-7
ISBN-13: 978-0-9792-2760-8
Copyright © 2006, Stone Age Institute Press.

All rights reserved under International and Pan-American Copyright Conventions. No part of this book may be reproduced or transmitted in any form or by any means, electronic or mechanical, including photocopying, without permission in writing from the publisher.

CHAPTER 12

THE BIOMECHANICS OF THE ARM SWING IN OLDOWAN STONE FLAKING

BY JESÚS DAPENA, WILLIAM J. ANDERST, AND NICHOLAS P. TOTH

ABSTRACT

The biomechanics of the arm swing in Oldowan stone flaking was analyzed using three-dimensional motion analysis methodology. The analysis calculated the joint torques (and therefore the dominant muscular actions) at the three main joints of the swinging arm.

The flexor, external rotator and abductor muscles of the shoulder and the flexor muscles of the elbow were activated by the subject after each impact to complete the braking of the downward motion of the hammerstone, and subsequently to speed up its upward motion. The extensor, internal rotator and adductor muscles of the shoulder and the extensor muscles of the elbow were then activated to slow down the upward motion of the hammerstone, and subsequently to accelerate its downward motion toward the core for the next impact.

The hammerstone traveled through a downward distance of 0.45-0.48 m, and reached a final velocity of 18.6-20.1 mph, which implied a kinetic energy equivalent to that of a baseball thrown at 39-42 mph. Since the archeological evidence indicates that Oldowan hominins were able to flake basalt cobbles very efficiently, it is probable that they achieved speed and kinetic energy values similar to those found in this study.

INTRODUCTION

A cursory examination of the motion of the swinging arm in stone flaking suggests that it should be clas-

sified as an “overarm” motion. This is a class of motions that includes a wide variety of human activities, such as hammering, baseball pitching, javelin throwing, tennis serving, water polo throwing, and football quarterback passing.

Sometimes the muscular actions that drive human motions seem evident. However, fast dynamic movements can be deceptive. For instance, in baseball pitching the elbow of the throwing arm extends at a very fast rate, but the elbow extensor musculature is not very active (Feltner & Dapena, 1986). The extension of the elbow is produced mainly by inertia through a rather complex flail-like mechanism driven by the shoulder musculature. This implies that a baseball pitcher needs great strength in the shoulder musculature but only moderate strength in the elbow extensor musculature. To find out the muscular actions that drive a human motion, it is necessary to use kinetic chain analysis.

In kinetic chain analysis, precise measurements of the motions of body segments are combined with information on the inertial parameters of those body segments (such as masses and moments of inertia) to calculate the force and the torque exerted by a body segment on its immediate distal neighbor. This force and this torque are exerted through the joint that connects the two segments, and therefore they are called the joint force and the joint torque. The joint force is the sum of all the forces exerted by muscles, bones, ligaments and other structures. It is generally not a very informative parameter. The joint torque is the sum of all the torques exerted about the center of the joint. Since these torques

are often exerted exclusively by muscles, the joint torque reflects the predominant muscular effort at the joint, and therefore it is a very informative parameter. The purpose of this project was to use kinetic chain analysis to determine the joint torques (and therefore the muscular actions) at the three main joints of the swinging arm during stone flaking.

METHODS

Calculation of Locations, Velocities and Accelerations

A skilled right-handed male (standing height = 1.75 m; mass = 75 kg) was filmed with two motion-picture cameras while he flaked lava cobbles. Both cameras were set at nominal frame rates of 200 frames/second. The cameras were placed to the right and in front of the subject, respectively.

Two typical trials (subsequently named Trial 1 and Trial 2) were selected for analysis. The film images were projected onto a digitizing tablet. The locations of 21 anatomical body landmarks (vertex, gonion, suprasternale, and right and left shoulders, elbows, wrists, knuckles, hips, knees, ankles, heels and toes) and of the approximate centers of the hammer and of the core were measured manually with the digitizing tablet in each film frame between an instant immediately after a stone impact and an instant immediately before the following stone impact. To minimize known problems in data acquisition in impact situations (see below), the trials were digitized only up to the last film frame prior to impact. The digitized locations taken from both cameras were stored in an Apple PowerBook G4 computer, which was also used for all subsequent calculations. (See Levanon & Dapena (1998) for further details on the methodology.)

The Direct Linear Transformation (DLT) method, developed by Abdel-Aziz & Karara (1971) and described in detail by Walton (1981), was used to compute the three-dimensional (3D) coordinates of the 23 landmarks from the digitized data. The 3D coordinates of the landmarks were expressed in terms of a right-handed orthogonal reference frame R1. The X1 and Y1 axes of R1 were horizontal, and perpendicular to each other; the Z1 axis was vertical, and pointed upward.

Coordinate data based on landmark locations obtained through manual digitization contain random errors that become magnified in the subsequent calculation of velocities and accelerations. To reduce this problem, the 3D location data were smoothed with quintic spline functions (Wood & Jennings, 1979) fitted to the time-dependent X_1 , Y_1 and Z_1 coordinates of each landmark. An appropriate degree of smoothing requires a compromise between two conflicting goals: the reduction of high frequency noise resulting from errors inherent in manual digitization, and the preservation of the true (lower frequency) patterns of the activity. For the

stone flaking trials, the best compromise was reached with a smoothing factor of $N \cdot 10 \cdot 10^{-6} \text{ m}^2$ for each landmark and direction, where N was the number of frames in the trial. (The smoothing factor determines the sum of squares of the differences between the smoothed coordinates and the raw coordinates; larger smoothing factors produce a greater amount of smoothing.) The first and second derivatives of the quintic spline functions yielded smoothed landmark velocity and acceleration values, respectively, in the X_1 , Y_1 and Z_1 directions.

Computation of Joint Torques

The swinging arm was modeled as a four-link kinetic chain composed of upper arm, forearm, hand, and hammerstone. The mass and the location of the center of mass (c.m.) of each arm segment in relation to its two endpoint landmarks were taken from Dempster's cadaver data (Dempster, 1955). Moment of inertia values were taken from Whitsett (1963), and were personalized for the subject using a procedure described by Dapena (1978). The mass of the hammerstone was determined with a scale ($m = 0.625 \text{ kg}$); the moment of inertia of the hammerstone about its own c.m. was assumed to be zero.

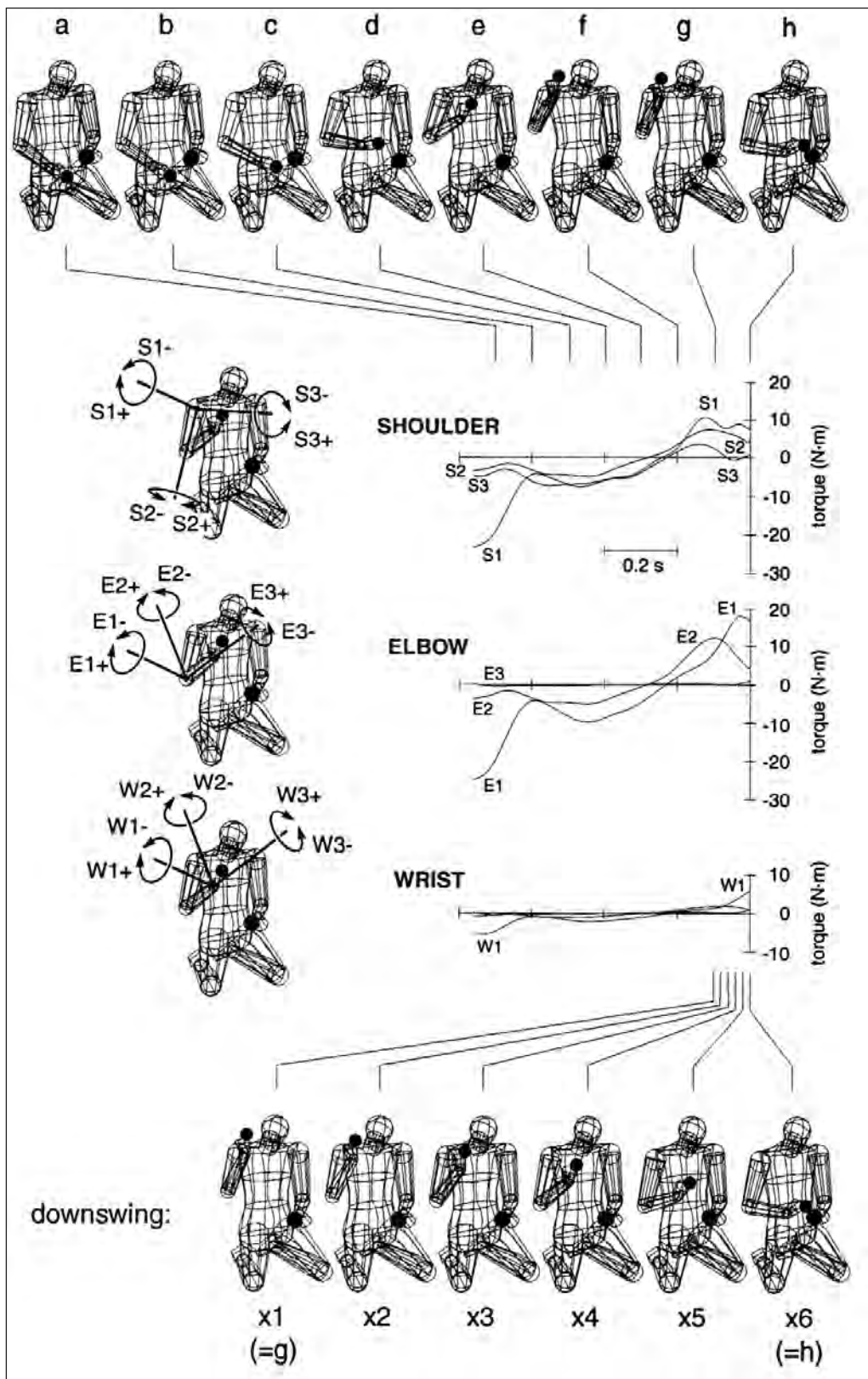
The hammerstone was assumed to be subjected to two forces: weight, acting at the c.m. of the stone, and a proximal force exerted by the hand through the c.m. of the stone. The hand was assumed to be subjected to the force of its own weight, the reaction to the force exerted by the hand on the stone, and a proximal joint force and a proximal joint torque exerted by the forearm on the hand at the wrist. The forearm and upper arm segments were each assumed to be subjected to the force of their own weight, acting through the c.m., plus a joint force and a joint torque at both the proximal and distal joints.

The instantaneous c.m. location and local angular momentum of each segment about its own c.m. were computed following procedures described by Dapena (1978), modified to use instantaneous landmark velocities. The net force exerted on each segment was calculated from the mass of the segment and the second derivative of its c.m. location. The net torque about the segment c.m. was computed as the first derivative of its angular momentum about its own c.m. A procedure described by Andrews (1974, 1982) was then used to calculate the force and torque exerted by the proximal segment on the distal segment at the shoulder, elbow and wrist joints.

Reference Frames for the Expression of Joint Torques

To aid in the interpretation of the joint torques, non-inertial orthogonal reference frames were defined for the shoulder, elbow and wrist joints. (See Figure 1.) The origin of reference frame R_3 was located at the shoulder joint. Axis S_1 was perpendicular to the plane formed by the longitudinal axes of the upper arm and forearm; S_2

Figure 1



1. Torques at the joints of the swinging arm in Trial 1. The computer graphics wireframe sequence at the top shows the entire stone-flaking cycle; the sequence at the bottom shows the downswing in greater detail. The wireframe drawings in the mid-left part of the Figure show the possible directions of the three torque components at each joint, and their signs. The plots show the values of the joint torques versus time. The wireframe sequences and patterns for trial 2 were similar to those of Trial 1.

was aligned with the longitudinal axis of the upper arm; S_3 was perpendicular to S_1 and S_2 . The origin of reference frame R_E was located at the elbow joint. Axis E_1 was perpendicular to the plane formed by the longitudinal axes of the upper arm and forearm (and was therefore parallel to S_1); E_2 was perpendicular to E_1 and to the longitudinal axis of the forearm; E_3 was aligned with the longitudinal axis of the forearm. The origin of reference frame R_W was located at the wrist joint. Its three axes, W_1 , W_2 and W_3 , were parallel to the corresponding axes of the R_E reference frame.

Problems with Data Smoothing in Activities Involving Impacts

The impact of the hammer against the core produces a sudden deceleration of the right arm. If pre-impact and post-impact data are included in the input to a smoothing program, the program will not be able to distinguish between the true acceleration (deceleration) produced by the impact and spurious accelerations due to noise in the data. Consequently, the data will be over-smoothed, and the deceleration produced by the impact will seem to start before the impact itself. This will add false “braking” torques at the shoulder, elbow and wrist joints prior to impact. To prevent such systematic errors, no post-impact data were input to the smoothing program. The locations, velocities and accelerations corresponding to the instant of impact were estimated by extrapolation from the quintic spline coefficients of the last time interval prior to impact.

RESULTS AND DISCUSSION

Stone Movements

The downward distance of travel of the hammerstone from its highest position to impact was 0.45-0.48 m in the two trials. The maximum speed of the hammerstone was 8.3-9.0 m/s (18.6-20.1 mph), and it occurred immediately before impact. This implied a kinetic energy of 21.5-25.3 Joules (J), equal to the kinetic energy of a baseball thrown at 39-42 mph. (For comparison, the kinetic energy of a baseball thrown by a major league pitcher at 90 mph is 117 J.) In both trials, the subject brought the core upward to meet the hammerstone at 0.6-1.3 m/s (1.3-2.9 mph). Although the motion of the core was not exactly opposite to the motion of the hammerstone, it contributed to increase the combined impact speed to 8.8-10.1 m/s (19.7-22.6 mph). Since the archeological evidence indicates that Oldowan hominins were able to flake basalt cobbles very efficiently, it is probable that they achieved speed and kinetic energy values similar to those found in this study.

Sequences

The wireframe sequence at the top of Figure 1 (images a-h) shows the complete cycle of the stone flaking action in Trial 1, from an instant shortly after the impact of the previous swing until the impact of Trial 1; the sequence at the bottom of the Figure (images x_1 - x_6) shows the downswing in greater detail. The sequences of Trial 2 were similar to those of Trial 1. The computer graphics sequences, as well as computer animations, showed that the motion of the swinging arm was not a simple planar flexion and extension, but a clear three-dimensional overarm motion.

Torques

The plots in the center-right section of Figure 1 show the torques at the three main joints of the right arm (shoulder, elbow and wrist). Joint torques give an indication of the muscular activity of the subject, and they occur in three different directions at each joint, as indicated by the images to the left of the plots. For instance, the negative E_1 torque in the early part of the cycle indicates that the elbow flexor muscles (such as the biceps) were dominant at that time, i.e., that the torque produced by the elbow flexor muscles about the center of the elbow joint was larger than any torque produced by the elbow extensor muscles (triceps); the positive E_1 torque in the late part of the cycle indicates that the elbow extensor muscles were dominant at that time. Two torques (E_2 at the elbow and W_3 at the wrist) are exceptions in that they are not produced by muscles; instead, they are passive torques exerted by the proximal segment on the distal segment through bony and ligamentous structures of the joint.

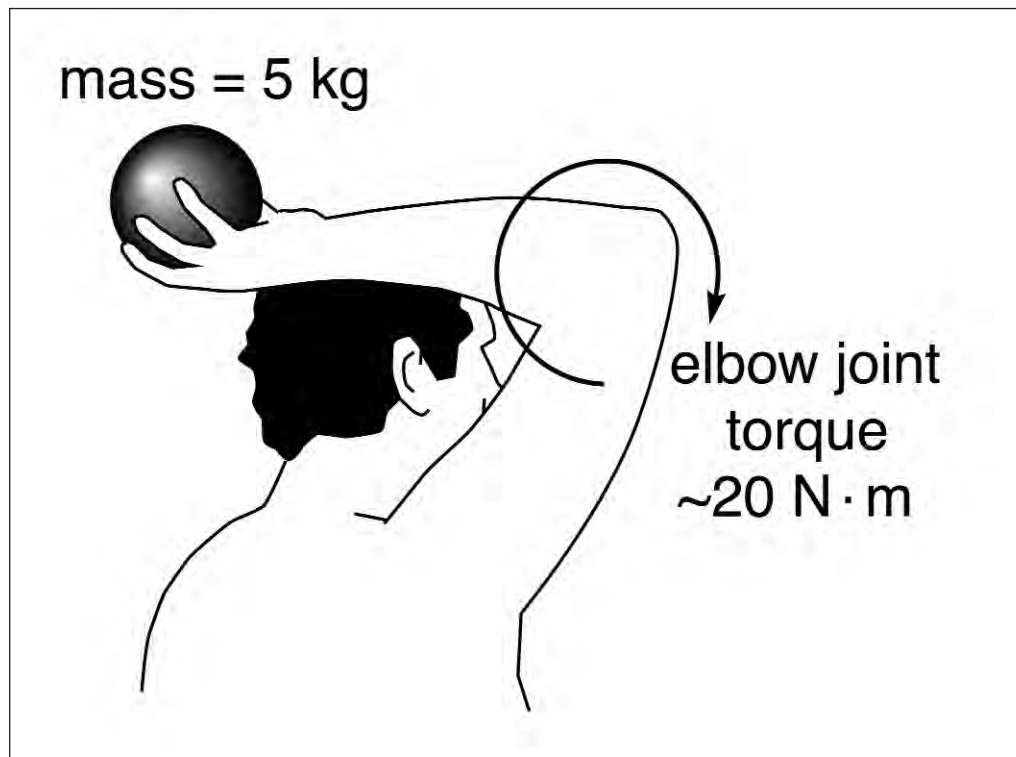
The torque plots indicate that in the early stages of the cycle (a-e) the shoulder muscles were active in the directions of flexion, external rotation and abduction (negative S_1 , S_2 and S_3 torques, respectively), while the elbow muscles were active in the direction of flexion (negative E_1 torque). These muscular actions served to stop the downward motion of the arm after the impact of the previous cycle (images a-b), and later to lift the upper arm and rotate it outward, and to flex the elbow (images b-e). About 0.25 seconds prior to impact, the torques reversed direction: The shoulder muscles became active in the directions of extension, internal rotation and adduction (positive S_1 , S_2 and S_3 torques, respectively), and the elbow muscles became active in the direction of extension (positive E_1 torque). These new muscular actions first stopped the upward and outward motion of the upper arm and the flexion of the elbow (images e-g), and then produced downward and inward rotation of the upper arm, and extension of the elbow (images g-h and x_1 - x_6). The muscles that cross the wrist joint did not play a major role in the generation of the arm swing. In contrast with baseball pitching, the torques of the flaking action were in good agreement with what might have been expected prior to the analy-

sis: The muscles that produce upward motion of the hammerstone were activated after the impact to complete the braking of the downward motion of the hammerstone, and subsequently to speed up its upward motion; the muscles that produce downward motion of the hammerstone were activated to slow down the upward motion of the hammerstone, and subsequently to accelerate its downward motion toward the core.

In comparison to the joint torques used in sports activities, the joint torques exerted by the shoulder and elbow muscles in stone flaking were relatively small. In a typical collegiate level baseball pitch, torques S_1 , S_2 and S_3 all reach maximum values of around $70 \text{ N} \cdot \text{m}$ (Feltner & Dapena, 1986), while the maximum shoulder torque values during the last 0.20 seconds prior to impact in the two flaking trials were: $S_1 = 11\text{-}14 \text{ N} \cdot \text{m}$;

$S_2 = 7\text{-}9 \text{ N} \cdot \text{m}$; $S_3 = 3\text{-}4 \text{ N} \cdot \text{m}$. The maximum elbow extension torque in the two flaking trials was $E_1 = 18\text{-}21 \text{ N} \cdot \text{m}$. This was not much smaller than the corresponding values in a typical baseball pitch ($20\text{-}30 \text{ N} \cdot \text{m}$), but it is important to bear in mind that the elbow extension torque is small in baseball pitching. For comparison purposes, it is useful to consider the fact that $20 \text{ N} \cdot \text{m}$ would be the approximate joint torque that the elbow extensor muscles would need to exert in order to hold up in the air a 5 kg load with the forearm in a horizontal position (Figure 2). This would be quite easy for most people. It is not surprising that stone flaking does not require a large amount of strength, since in prehistoric times this activity probably needed to be accessible to a large number of individuals.

Figure 2



2. Elbow joint torque necessary to hold a 5 kg mass up in the air.

REFERENCES CITED

- Abdel-Aziz, Y.I. and H.M. Karara. Direct linear transformation from comparator coordinates into object space coordinates in close-range photogrammetry. In: *Proceedings of ASP/UI Symposium on Close Range Photogrammetry*, Falls Church, VA: American Society of Photogrammetry, pp. 1-18, 1971.
- Andrews, J.G. Biomechanical aspects of human motion. In: *Kinesiology IV*, Washington, D.C.: American Association for Health, Physical Education and Recreation, pp. 32-42, 1974.
- Andrews, J.G. On the relationship between resultant joint torques and muscular activity. *Med. Sci. Sports Exerc.* 14:361-367, 1982.
- Dapena, J. A method to determine the angular momentum of a human body about three orthogonal axes passing through its center of gravity. *J. Biomechanics* 11:251-256, 1978.
- Dempster, W.T. Space requirements of the seated operator. *WADC Technical Report 55-159*, Dayton, OH: Wright-Patterson Air Force Base, 1955.
- Feltner, M.E. and J. Dapena. Dynamics of the shoulder and elbow joints of the throwing arm during a baseball pitch. *Int. J. Sport Biomechanics* 2:235-259, 1986.
- Levanon, J. and J. Dapena. Comparison of the kinematics of the full-instep and pass kicks in soccer. *Med. Sci. Sports Exerc.* 30:917-927, 1998.
- Walton, J.S. Close range cine photogrammetry: a generalized technique for quantifying human motion. Ph.D. Dissertation, Pennsylvania State University, University Park, PA, 1981.
- Whitsett, C.E. Some dynamic response characteristics of weightless man. *AMRL Technical Report 18-63*, Dayton, OH: Wright-Patterson Air Force Base, 1963.
- Wood, G.A. and L.S. Jennings. On the use of spline functions for data smoothing. *J. Biomechanics* 12:477-479, 1979.